



## Ultrathin Polyimide Coating for a Spinel $\text{LiNi}_{0.5}\text{Mn}_{1.5}\text{O}_4$ Cathode and Its Superior Lithium Storage Properties under Elevated Temperature Conditions

M. C. Kim,<sup>a</sup> S. H. Kim,<sup>a</sup> V. Aravindan,<sup>b</sup> W. S. Kim,<sup>c</sup> S. Y. Lee,<sup>d,z</sup> and Y. S. Lee<sup>a,z</sup>

<sup>a</sup>Faculty of Applied Chemical Engineering, Chonnam National University, Gwang-ju 500-757, Korea

<sup>b</sup>Energy Research Institute @ NTU (ERI@N), Nanyang Technological University, Singapore 637553

<sup>c</sup>Daejung EM Co. Ltd, Incheon 405-820, Korea

<sup>d</sup>Interdisciplinary School of Green Energy, Ulsan National Institute of Science and Technology, Ulsan, 689-798 Korea

In this study, we present the influence of polyimide (PI) coating concentration on the electrochemical properties of high voltage, spinel phase  $\text{LiNi}_{0.5}\text{Mn}_{1.5}\text{O}_4$  cathodes, particularly under elevated temperature conditions. First, the adipic acid-mediated sol-gel technique was employed to synthesize sub-micron sized  $\text{LiNi}_{0.5}\text{Mn}_{1.5}\text{O}_4$  particles, where Mn was in the 4+ state. Thermal polymerization was used to produce the PI coating from polyamic acid. The presence of the PI layer was confirmed by transmission electron microscopy and Fourier-transform infrared analyses. All test cells delivered good cycleability under ambient temperature conditions, irrespective of the PI coating concentration, with a prominent plateau at 4.7 V vs. Li, whereas all test cells experienced the poorest electrochemical behavior under elevated temperature conditions except 0.3 wt.% PI. The 0.3 wt.% PI coated  $\text{LiNi}_{0.5}\text{Mn}_{1.5}\text{O}_4$  phase delivered excellent cycleability with capacity retention of > 90% at 55°C. Poor compatibility and severe reactivity toward the electrolyte solution resulted in the poorest performance which was clearly evidenced by the scanning electron microscopy analysis and supported well by impedance studies after galvanostatic cycling.

© 2013 The Electrochemical Society. [DOI: 10.1149/2.013308jes] All rights reserved.

Manuscript submitted February 20, 2013; revised manuscript received April 15, 2013. Published April 25, 2013.

The development of Li-ion batteries (LIB) with high energy densities has attracted much attention, as such power packs are anticipated to drive hybrid electric vehicles (HEV) and electric vehicles (EV) in the near future.<sup>1-4</sup> However, the development of such LIBs completely relies on the utilization of high voltage cathode candidates such as  $\text{LiCoPO}_4$  (~4.8 V vs. Li),  $\text{Li}_2\text{CoPO}_4\text{F}$  (~5 V vs. Li), and the metal doped spinels  $\text{LiM}_x\text{Mn}_{2-x}\text{O}_4$ , (M=Co, Cr, Ni, Fe, Cu, etc. (~4.7 V vs. Li)).<sup>2,3,5,6</sup> Among them, polyanion framework materials  $\text{LiCoPO}_4$  and  $\text{Li}_2\text{CoPO}_4\text{F}$  include the toxic and expensive transition metal Co, which increases safety concerns and production costs.<sup>7</sup> In addition, the  $\text{PO}_4^{3-}$  anion dissolves in the carbonate-based electrolyte of a  $\text{LiCoPO}_4$  cathode.<sup>8-10</sup> Extracting two moles of Li is still not possible due to the restricted thermodynamic stability window of the carbonate-based electrolyte (~4.6 V vs. Li).<sup>6</sup> In addition, a  $\text{Co}^{2+/3+}$  redox couple occurs at ~5 V vs. Li, which results in severe capacity fading during the cycle.<sup>6,11</sup> Hence, research focus has been directed toward utilizing transition metal doped spinels, particularly Ni doped spinels ( $\text{LiNi}_{0.5}\text{Mn}_{1.5}\text{O}_4$ ), because the redox potential is slightly lower than the former polyanion framework candidates, it has a lower cost, and is eco-friendly.<sup>5,12-14</sup> Electrolyte decomposition is another important issue for all of the aforementioned materials, and there are few reports available on the electrochemical performance of the spinel  $\text{LiNi}_{0.5}\text{Mn}_{1.5}\text{O}_4$  phase. Elevated temperature performance is another important criterion to employ LIBs in HEV and EV applications, in which Mn dissolves at high temperature.<sup>1,5,15</sup> Hence, surface modification is necessary to prevent Mn dissolution and promote high temperature performance. To date, several surface modifications such as carbon and metal oxide coatings have been used to improve the electrochemical performance of  $\text{LiNi}_{0.5}\text{Mn}_{1.5}\text{O}_4$ , which requires additional heat treatment to enable such coatings. Nevertheless, such additional heat treatment may affect structural properties. A metal oxide coating ( $\text{ZrO}_2$ ,  $\text{ZnO}$ , etc) results in a heterogeneous covering of the active particulates, whereas a carbon coating leads to a decrease in volumetric capacity irrespective of the testing temperature.<sup>16-18</sup> Another way to protect the active material is to encapsulate the polymeric molecules. Protecting active particles with conducting polymers (polyaniline, polypropylene, poly(3,4-ethylenedioxythiophene), polyimide [PI] etc.) is attractive without compromising volumetric capacity unlike a carbon coating.<sup>19-22</sup> Among them, PI has been widely used as a dielectric medium in transistor applications, liquid crystal displays, and membranes due to its outstanding mechanical, thermal,

and chemical stability as well as film forming abilities. In our previous study, we successfully demonstrated improved electrochemical properties of layered type  $\text{LiCoO}_2$  cathodes during high voltage charging (4.4 V vs. Li). In addition, improvement in the thermal properties of about ~15°C was observed in the charged state (4.4 V vs. Li).<sup>20</sup> In this study, we attempted to encapsulate the  $\text{LiNi}_{0.5}\text{Mn}_{1.5}\text{O}_4$  particles with various concentrations of PI. As mentioned earlier, elevated temperature performance is the main setback for  $\text{LiNi}_{0.5}\text{Mn}_{1.5}\text{O}_4$  cathodes, therefore we are very much interested to improve the elevated temperature performance by adopting PI coating by in-situ thermal polymerization process. In this line, the  $\text{LiNi}_{0.5}\text{Mn}_{1.5}\text{O}_4$  particles were first prepared using conventional sol-gel method to yield a single phase material. The PI decorated  $\text{LiNi}_{0.5}\text{Mn}_{1.5}\text{O}_4$  particles were tested under both ambient and elevated temperature conditions, and the influence of PI concentration on the structural, morphological, and electrochemical properties was investigated and described.

### Experimental

The conventional sol-gel method was adopted to synthesize the spinel phase  $\text{LiNi}_{0.5}\text{Mn}_{1.5}\text{O}_4$  powder described in our previous study.<sup>23</sup> In a typical synthesis procedure, all analytical grade starting materials such as  $\text{Li}(\text{CH}_3\text{COO}) \cdot \text{H}_2\text{O}$  (Junsei Chem, Tokyo, Japan),  $\text{Ni}(\text{CH}_3\text{COO}) \cdot 4 \text{H}_2\text{O}$  (Aldrich, St. Louis, MO, USA), and  $\text{Mn}(\text{CH}_3\text{COO}) \cdot 4 \text{H}_2\text{O}$  (Aldrich) were dissolved separately in a molar ratio in distilled water. Then, they were mixed together along with the  $\text{C}_6\text{H}_{10}\text{O}_4$  chelating agent (adipic acid, Sigma-Aldrich) and stirred continuously at 90°C until the precursor powder was obtained. The precursor powder was pre-calcined at ~450°C for 10 h to decompose the acetate moieties. The intermediate product was harvested and prepared as a pellet again to sinter at 700°C for 12 h to yield the single-phase  $\text{LiNi}_{0.5}\text{Mn}_{1.5}\text{O}_4$  powder. The PI coating process was thermally conducted by in situ polymerization of a polyamic acid solution. Various concentrations of polyamic acid were used, in which the active particles were dispersed, continuously stirred for 10 min, and then filtered. The filtered powder was dried at 30°C for 1 h and then vacuum-dried at 30°C for 4 h. Conversion of polyamic acid to PI was carried out by a stepwise thermal imidization process (60°C for 30 min → 120°C for 30 min → 200°C for 60 min → 300°C for 60 min → 400°C for 10 min under nitrogen atmosphere).<sup>20</sup>

Structural properties were evaluated using an X-ray diffractometer (Rint 1000, Rigaku, Tokyo, Japan) equipped with a  $\text{Cu K}_\alpha$  radiation source. The surface morphology of the powder was analyzed

<sup>z</sup>E-mail: syleek@unist.ac.kr; leeys@chonnam.ac.kr

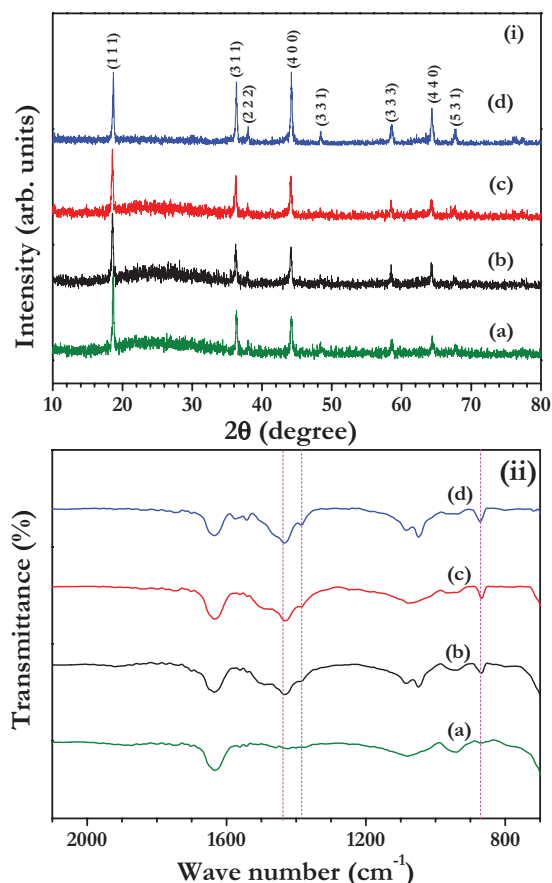


**Figure 1.** (i) Powder X-ray diffraction pattern of spinel phase  $\text{LiNi}_{0.5}\text{Mn}_{1.5}\text{O}_4$  cathodes with various concentrations of polyimide (a) 0, (b) 0.3, (c) 0.5, and (d) 1%; and (ii) Fourier transform infrared spectra of various concentrations of polyimide coated  $\text{LiNi}_{0.5}\text{Mn}_{1.5}\text{O}_4$  (a) 0, (b) 0.3, (c) 0.5, and (d) 1 wt.%.

by field emission scanning electron microscopy (FE-SEM, S4700, Hitachi, Tokyo, Japan). The internal structure of the powder was studied using transmission electron microscopy (TEM, TECNAI, Philips, The Netherlands). Fourier transform-infrared (FT-IR) spectroscopic measurements were carried out (IR spectrometer Presitge-21, Tokyo, Japan). The electrochemical studies were performed in a two electrode CR 2032 coin-cell assembly. The composite electrodes were fabricated with 20 mg of accurately weighed active materials, 3 mg conductive additive (super P), and 3 mg of teflonized acetelene black (TAB-2) using ethanaol as the solvent. The resulting film was pressed on a 200 mm<sup>2</sup> stainless steel mesh that served as a current collector. The test cells were fabricated with a composite cathode and a metallic lithium anode, which was separated by porous polypropylene film (Celgard 3401, Dallas, TX, USA). A 1 M  $\text{LiPF}_6$  solution in ethylene carbonate: dimethyl carbonate (1:1 by vol., Solbrain Co., Ltd., Seoul, Korea) was used as the electrolyte without any further purification. Cyclic voltammetry (CV) and electrochemical impedance spectroscopic (EIS) studies were conducted in a two-electrode setup using a Bio-Logic electrochemical work station (SP-150, Biologic, Claix, France), in which metallic lithium served as both the counter and reference electrode. Galvanostatic cycling studies were carried out at 3.5–5 V vs. Li under ambient and elevated temperature (55°C) conditions.

## Results and Discussion

The X-ray diffraction (XRD) patterns of the PI-coated  $\text{LiNi}_{0.5}\text{Mn}_{1.5}\text{O}_4$  powder are given in Fig. 1(i). Note the presence of a single phase material without any impurity traces, particularly in the

$\text{Li}_x\text{Ni}_{1-x}\text{O}$  phases. The observed reflection can be indexed to the spinel phase with a  $Fd\bar{3}m$  space group, in which the Li ions are located at 8a sites, the Mn and Ni ions are randomly distributed at 16d sites, and the O ions occupy the 32e sites.<sup>5,12</sup> Furthermore, FT-IR spectra also supported the formation of the  $Fd\bar{3}m$  space group. No additional peaks were noted for the PI coated spinel  $\text{LiNi}_{0.5}\text{Mn}_{1.5}\text{O}_4$ , indicating that the polymer coating i.e. PI coating did not affect the structural properties of the native phase since the material is subjected to thermal treatment during the polymerization process. However, it was difficult to confirm the presence of the PI layer over the surface of  $\text{LiNi}_{0.5}\text{Mn}_{1.5}\text{O}_4$  using XRD, as too small an amount of PI was coated only over the active particulate surface. Hence, FT-IR was adopted to validate the presence of PI, and the results are given in Fig. 1b. The appearance of new bands at ~1385, 1436, and 868 cm<sup>-1</sup> confirmed cross linking of the imide group, the stretching mode (C–N) of the imide group, and the out of plane bending vibrations of  $\text{C}_6\text{H}_3$ , respectively, for the PI coated powders.<sup>24</sup> The presence of such new bands indicated the PI along with spinel phase  $\text{LiNi}_{0.5}\text{Mn}_{1.5}\text{O}_4$  irrespective of concentration.

The surface morphological features of the PI coated spinel phase  $\text{LiNi}_{0.5}\text{Mn}_{1.5}\text{O}_4$  powder were analyzed by FE-SEM and are illustrated in Fig. 2. Native compounds exhibited a fine particulate morphology with an average size of ~100 nm (Fig. 2a). When PI was introduced, the particles tended to aggregate weakly during the polymerization process from polyamic acid to PI i.e. various thermal treatment steps. The aggregation was more severe at higher PI (1 wt.%) concentrations compared to that at lower concentrations (0.3 wt.%). However, particulate morphology was beneficial to formulate good quality electrodes. Therefore, high performance is anticipated for the sol-gel derived spinel phase  $\text{LiNi}_{0.5}\text{Mn}_{1.5}\text{O}_4$  powder. High resolution-TEM was performed to establish the presence of the PI layer over the active particles (Fig. 3). Only selected PI coated samples were subjected to investigation such as the 0.3 wt.% PI coated  $\text{LiNi}_{0.5}\text{Mn}_{1.5}\text{O}_4$ . Very clear lattice fringes were noted on the edges of the native phase  $\text{LiNi}_{0.5}\text{Mn}_{1.5}\text{O}_4$  compounds, whereas a ~2 nm amorphous layer was found on the PI coated powders. The observed layer was thermally polymerized PI.

Li-insertion properties were investigated in half-cell configurations at 3.5–5 V vs. Li and a current density of 0.2 mA cm<sup>-2</sup> under ambient temperature conditions and are presented in Fig. 4. Figure 4a presents the typical charge-discharge curves of the spinel phase  $\text{LiNi}_{0.5}\text{Mn}_{1.5}\text{O}_4$  compounds. A long distinct plateau at ~4.7 V vs. Li was observed for all samples investigated, which corresponded to the  $\text{Ni}^{2+/4+}$  redox couple.<sup>24</sup> However, the deviation in the curve/appearance of the plateau at about ~4 V vs. Li was due to the trace amount of  $\text{Mn}^{3+}$  present in the spinel phase and was associated with the  $\text{Mn}^{3+/4+}$  redox couple. No deviation was noted for the native phase compound, indicating that the Mn atoms were in the 4+ state. However, thermal polymerization slightly reduced the  $\text{Mn}^{4+}$  to  $\text{Mn}^{3+}$ . Additionally, the observed traces were consistent with the ordered Ni doped spinel reported by Zaghbi et al. using wet chemical synthesis.<sup>25</sup> The test cells delivered discharge capacities of ~138, ~113, ~115, and ~92 mAh g<sup>-1</sup> for 0, 0.3, 0.5, and 1 wt.% concentrations of PI, respectively. When the concentration was increased from 0 to 1 wt.%, polarization of the electrodes tended to increase, which resulted in a decrease in the discharge capacity values. However, there was only a marginal difference between the polarization of the electrodes for the 0.3 and 0.5 wt.% concentrations of PI. The increase in polarization of the electrode was expected, as PI has good electronic insulating properties and poor compatibility with decomposition of the electrolyte solution. The possible dissolution of  $\text{Mn}^{3+}$  ions cannot be excluded for such fading.<sup>15</sup> The plots of the cycling profiles for the PI coated samples recorded at ambient temperatures are illustrated in Fig. 4b. A decrease in the specific capacity profiles were noted for native phase compounds compared to the PI decorated  $\text{LiNi}_{0.5}\text{Mn}_{1.5}\text{O}_4$  phases. The cell retained 89, 98, and 96% of its initial capacity after 70 cycles for 0, 0.3, and 0.5% of PI, respectively whereas slightly increasing capacity profiles were observed for 1% PI. Although the 1% PI coated powder delivered lower capacity values, it had excellent cycleability compared to that of the remaining concentrations.

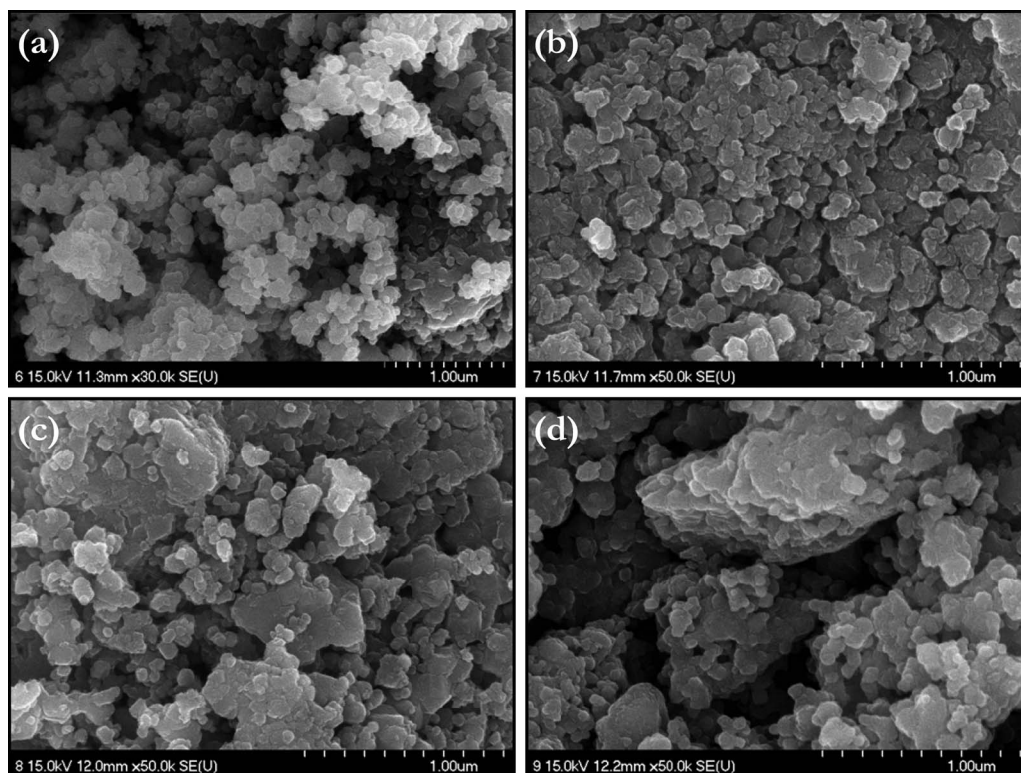


**Figure 2.** Scanning electron microscopic images of spinel phase  $\text{LiNi}_{0.5}\text{Mn}_{1.5}\text{O}_4$  cathodes with various concentrations of polyimide coating (a) 0, (b) 0.3, (c) 0.5, and (d) 1 wt. %.

Cycling voltammograms were recorded for native and 0.3 wt. % PI coated  $\text{LiNi}_{0.5}\text{Mn}_{1.5}\text{O}_4$  powder in the half-cell configuration at 3.2–5 V vs. Li and a slow scan rate of  $0.2 \text{ mV s}^{-1}$  under ambient temperature conditions and are presented in Fig. 5. A strong anodic peak was observed at  $\sim 4.9 \text{ V}$  vs. Li and was attributed to the  $\text{Ni}^{2+/4+}$  redox couple. Variations in current densities were noted between the native and 0.3 wt. % PI coated  $\text{LiNi}_{0.5}\text{Mn}_{1.5}\text{O}_4$  material, although they were loaded with 20 mg of active material. The reduction in the area underneath the curve for the 0.3 wt. % PI coated  $\text{LiNi}_{0.5}\text{Mn}_{1.5}\text{O}_4$  material indicated the lower capacity profile and was consistent with the galvanostatic profiles observed in Fig. 3. No obvious peaks were noted at  $\sim 4 \text{ V}$  vs. Li for the native phase, clearly indicating the presence of  $\text{Mn}^{4+}$ , whereas very small intense peaks were observed

for the 0.3 wt. % PI coated  $\text{LiNi}_{0.5}\text{Mn}_{1.5}\text{O}_4$ . This clearly shows that the thermal polymerization process leads to the formation of a trace amount of  $\text{Mn}^{3+}$  ions. The observed CV traces were consistent with galvanostatic cycling profiles and a report by Zaghbi et al.<sup>25</sup>

Elevated temperature is one of the main criteria to develop high performance Li-ion power packs to employ them in HEV and EV applications.<sup>3</sup> However, the main setback associated with spinel phase  $\text{LiNi}_{0.5}\text{Mn}_{1.5}\text{O}_4$  material is that Mn dissolution occurs severely along with electrolyte decomposition which results in severe capacity fading. It is well known that,  $\text{LiPF}_6$  is thermally unstable and decomposes to LiF and  $\text{PF}_5$  in a reaction that is accelerated in the presence of organic molecules. Then,  $\text{PF}_5$  hydrolyzes to form HF and  $\text{PF}_3\text{O}$ , which react with cathode active particles and dissolve the active particulates

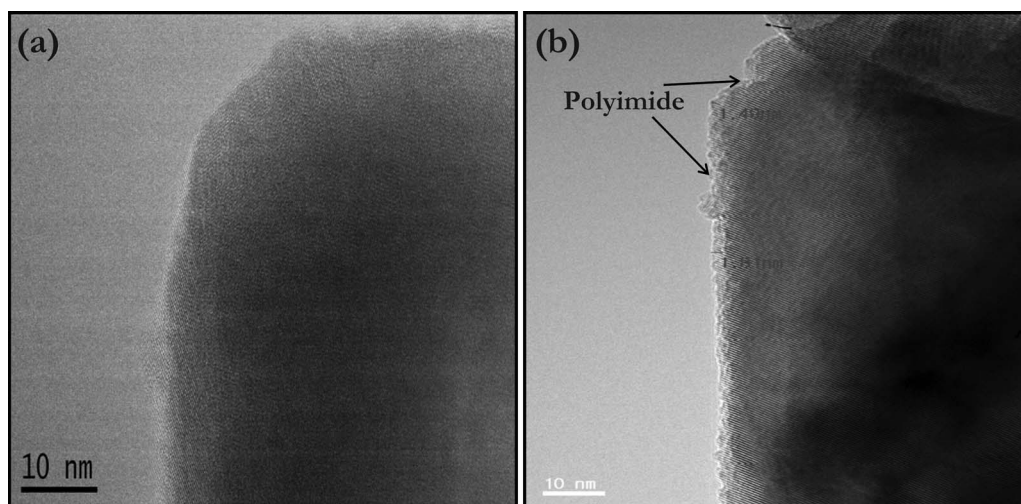


**Figure 3.** High resolution transmission electron microscopic images of (a) 0 and (b) 0.3 wt. % polyimide coated  $\text{LiNi}_{0.5}\text{Mn}_{1.5}\text{O}_4$ .

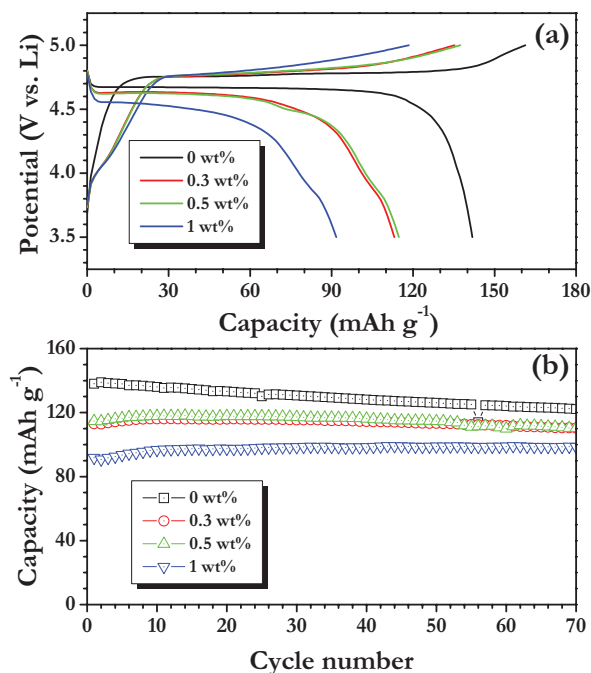


**Figure 4.** Galvanostatic charge-discharge profiles of spinel phase  $\text{LiNi}_{0.5}\text{Mn}_{1.5}\text{O}_4$  cathodes with various concentrations of polyimide coating in half-cell assembly recorded at 3.5–5 V vs. Li and a current density of  $0.2 \text{ mA cm}^{-2}$  in ambient temperature, (a) typical charge-discharge curves and (b) plot of discharge capacity vs. cycle number.

subsequently deteriorating cell performance.<sup>26</sup> All of the PI coated spinel phase  $\text{LiNi}_{0.5}\text{Mn}_{1.5}\text{O}_4$  powders were subjected to high temperature ( $55^\circ\text{C}$ ) cycling in the half-cell configuration at 3.5–5 V vs. Li and a current density of  $0.2 \text{ mA cm}^{-2}$  (Fig. 6). As expected, the test cells delivered a higher capacity profile than those at ambient temperature conditions. For example, reversible capacity of 138, 117, 128, and  $104 \text{ mAh g}^{-1}$  was observed for the 0, 0.3, 0.5 and 1 wt.% concentrations of PI, respectively. The cycling profiles for the PI coated spinel phase materials are given in Fig. 6b. The difference between the electrochemical properties of PI coated spinel phase  $\text{LiNi}_{0.5}\text{Mn}_{1.5}\text{O}_4$  powders is apparent. Very severe capacity fading was encountered for all compositions, except 0.3 wt.%. The test cells retained  $\sim 19$ ,  $\sim 90$ ,  $\sim 9$ , and  $\sim 25\%$  of initial discharge capacity after 60 galvanostatic

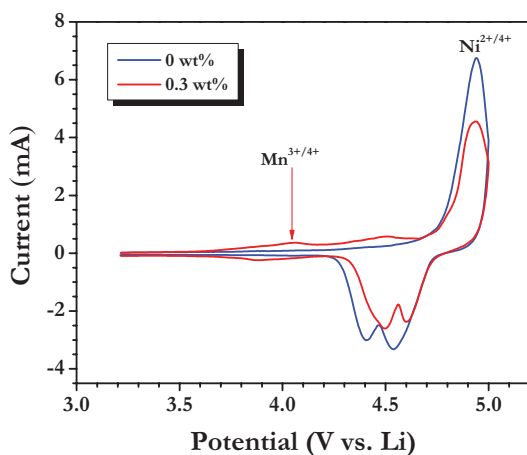


**Figure 5.** Cyclic voltammograms of polyimide coated spinel phase  $\text{LiNi}_{0.5}\text{Mn}_{1.5}\text{O}_4$  in a half-cell assembly and recorded at 3.5–5 V vs. Li and a slow scan rate of  $0.2 \text{ mV s}^{-1}$  under ambient temperature conditions.

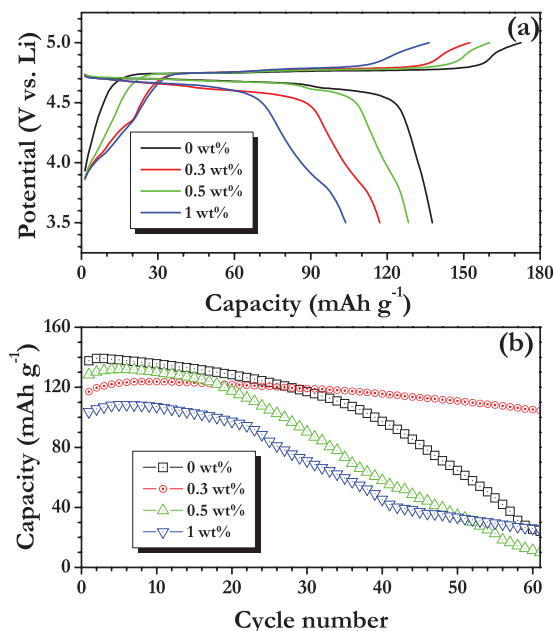


**Figure 6.** Galvanostatic charge-discharge profiles of spinel phase  $\text{LiNi}_{0.5}\text{Mn}_{1.5}\text{O}_4$  cathodes with various concentrations of polyimide coating in half-cell assembly tested at 3.5–5 V vs. Li and a current density of  $0.2 \text{ mA cm}^{-2}$  under elevated temperature ( $55^\circ\text{C}$ ), (a) typical charge-discharge curves and (b) plot of discharge capacity vs. cycle number.

cycles for the 0, 0.3, 0.5, and 1 wt.% concentrations of PI, respectively. Fading was observed compared to native phase at higher concentrations of the PI coating. This was possibly due to the heterogeneous coating originating from aggregation during thermal polymerization of PI, which was clearly evident from the FE-SEM observations (Fig. 2). Such aggregation results in severe reactivity of the electrolyte and leads to the formation of polymeric and inorganic by-products over the surface of the active particulates and become an inactive mass that impedes ionic migration.<sup>26,27</sup> This gradually reduces the participation of active particles during electrochemical reaction in successive cycles and leads to capacity fading. The presence of such a homogeneous PI layer over the surface of active particles hinders the direct reaction between the  $\text{LiNi}_{0.5}\text{Mn}_{1.5}\text{O}_4$  powder and the electrolyte solution, which resulted in the improved battery performance for the 0.3 wt.% concentration PI.

A post-mortem analysis was carried out to validate the severe reactivity of  $\text{LiNi}_{0.5}\text{Mn}_{1.5}\text{O}_4$  particles toward electrolyte solution and is given in Fig. 7. Figure 7a and 7c show the surface morphology of native and 0.3 wt.% PI coated  $\text{LiNi}_{0.5}\text{Mn}_{1.5}\text{O}_4$  composite electrodes, which clearly show that the particulate morphology is consistent with the synthesized powder given in Fig. 2. Severe reactivity of the native phase compound toward the electrolyte solution was noted, which resulted in transition metal dissolution that influenced the morphological features (Fig. 7c). A highly melted rock-like morphology was observed for such native compounds after 60 galvanostatic cycles under an elevated temperature condition, whereas the particulate morphology was retained for 0.3 wt.% PI coated phase (Fig. 7b and 7d). This clearly showed the protective nature of the PI layer for high voltage spinel phase  $\text{LiNi}_{0.5}\text{Mn}_{1.5}\text{O}_4$  cathodes under elevated temperature conditions.

EIS was employed before and after cycling (60 cycles at elevated temperature conditions) to qualitatively study the influence of the PI coating on  $\text{LiNi}_{0.5}\text{Mn}_{1.5}\text{O}_4$  particles (Fig. 8). The Nyquist plots were recorded in two electrode half-cell configurations, which provides information about conductivity, dielectric coefficient, static properties of the interfaces, and its dynamic change due to adsorption or charge-transfer phenomena. Nyquist plots comprising the three main regions are clearly shown in Fig. 8. The presence of a high-frequency

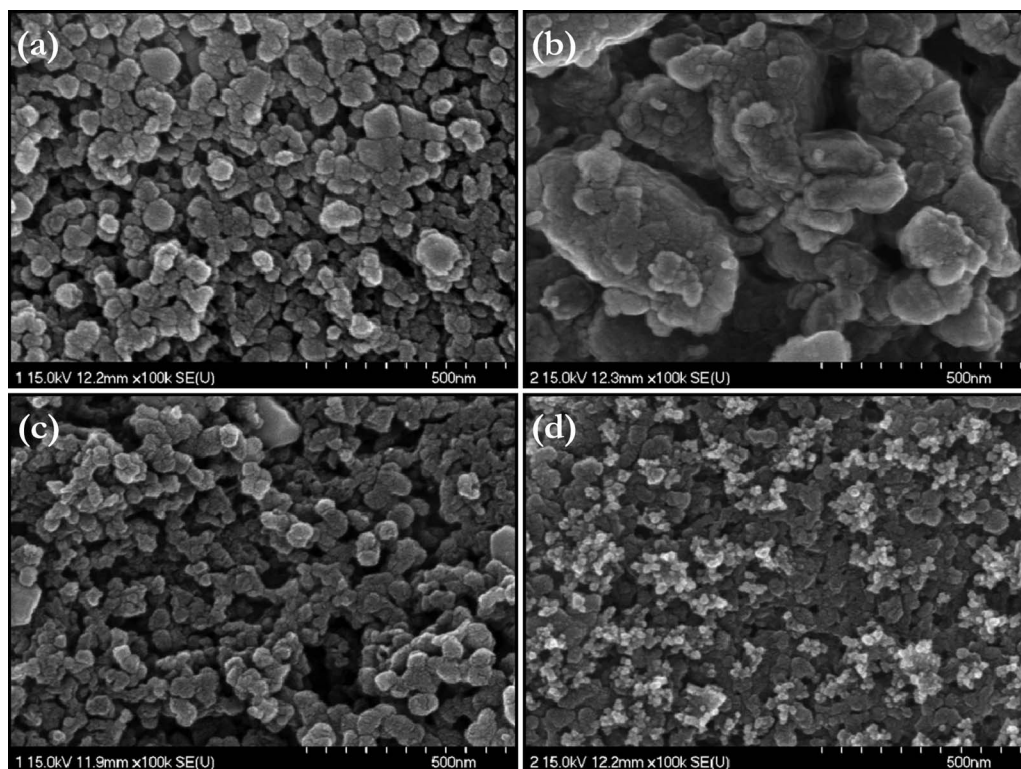


**Figure 7.** Scanning electron microscopic images of spinel phase  $\text{LiNi}_{0.5}\text{Mn}_{1.5}\text{O}_4$  materials before and after cycling at elevated temperature ( $55^\circ\text{C}$ ) (a) & (b) before and after cycling of native phase compound, (c) & (d) before and after cycling of the 0.3 wt.% polyimide coating.

semicircle is attributed to the formation of a solid electrolyte interface film and/or contact resistance, the medium frequency region was correlated to the charge-transfer (CT) impedance across the electrode/electrolyte interface, and the vertical tail inclined approximately  $45^\circ$  toward the real axis indicates the lithium diffusion kinetics and is called a Warburg tail.<sup>28</sup> The inset shows the Nyquist plot of the EIS traces before galvanostatic cycling and the resistance at  $\sim 5\ \Omega$  was ascribed to the solution/electrolyte resistance. However, no much variation in CT resistance was noted ( $\sim 23\ \Omega$ ), which is generally used to describe the conducting properties of an electrode material. There-

fore, the PI modification did not influence the electronic conducting properties of the spinel phase material. In contrast, huge variations in the CT values were noted after 60 galvanostatic cycles. The CT resistance of  $\sim 546$  and  $\sim 242\ \Omega$  was noted for native and 0.3 wt.% PI coated  $\text{LiNi}_{0.5}\text{Mn}_{1.5}\text{O}_4$  electrodes. The drastic variation in CT resistance for native phase  $\text{LiNi}_{0.5}\text{Mn}_{1.5}\text{O}_4$  corresponded to the severe reactivity toward the electrolyte counterpart and subsequent formation of inorganic and polymeric by-products over the surface of active particulates. However, relatively small reactivity was noted for the 0.3 wt.% PI coated  $\text{LiNi}_{0.5}\text{Mn}_{1.5}\text{O}_4$  powder compared to that of the native compound and this paralleled the FE-SEM results observed after galvanostatic cycling (Fig. 6). This PI coating study certainly provides a method to increase the electrochemical performance of cathode materials under high temperature cycling by employing a simple polymer coating. This technique can be easily extended for other cathode materials.

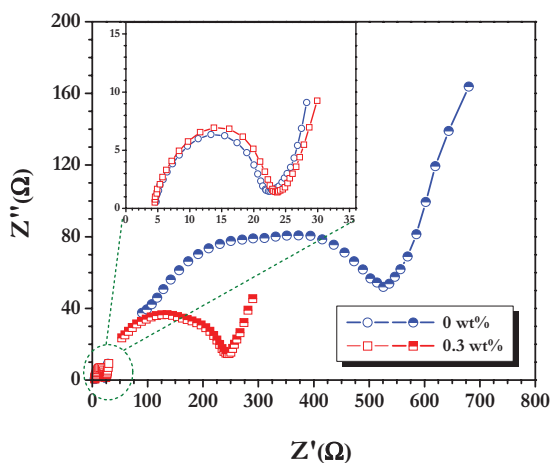


**Figure 8.** Electrochemical impedance spectra of spinel phase  $\text{LiNi}_{0.5}\text{Mn}_{1.5}\text{O}_4$  materials (0 and 0.3 wt.% polyimide coated) recorded after 60 cycles. Magnified Nyquist plot shows the EIS traces recorded before conducting galvanostatic cycling at  $55^\circ\text{C}$ .

## Conclusions

Elevated temperature performance of a high voltage spinel phase  $\text{LiNi}_{0.5}\text{Mn}_{1.5}\text{O}_4$  cathode was substantially enhanced by PI coating through thermal polymerization of polyamic acid. The influence of the PI coating on the electrochemical properties was studied under both ambient and elevated temperature conditions ( $55^\circ\text{C}$ ). Increasing the PI concentration tended to increase polarization of the electrodes which resulted in a decrease in specific capacity values. The test cells rendered good cycleability under ambient temperature conditions, irrespective of the PI coating in the half-cell assembly. At elevated temperature conditions, the 0.3 wt.% PI coated  $\text{LiNi}_{0.5}\text{Mn}_{1.5}\text{O}_4$  delivered excellent cycleability and retained  $\sim 90\%$  of its initial capacity after 60 cycles. Poor cycleability of the remaining materials was mainly due to severe reactivity toward the electrolyte solution and subsequent dissolution of the transition metals present in the cathode. The said reaction was clearly evidenced from a post-mortem

analysis and qualitatively supported by impedance measurements. This PI coating will pave the way to improve the electrochemical performance at elevated temperature conditions and increase the possibility of using high power Li-ion power packs for HEV and EV applications.

### Acknowledgments

This study was supported by the IT R&D program of MKE/KEIT. [KI10039182, Development of 5 V cathode material which capacity is 125 mAh g<sup>-1</sup> & high voltage electrolyte which decomposition is over 5 V for lithium secondary battery]

### References

1. V. Aravindan, J. Gnanaraj, Y.-S. Lee, and S. Madhavi, *Journal of Materials Chemistry A*, **1**, 3518 (2013).
2. N.-S. Choi, Z. Chen, S. A. Freunberger, X. Ji, Y.-K. Sun, K. Amine, G. Yushin, L. F. Nazar, J. Cho, and P. G. Bruce, *Angewandte Chemie International Edition*, **51**, 9994 (2012).
3. E. J. Cairns and P. Albertus, *Annual Review of Chemical and Biomolecular Engineering*, **1**, 299 (2010).
4. C. M. Hayner, X. Zhao, and H. H. Kung, *Annual Review of Chemical and Biomolecular Engineering*, **3**, 445 (2012).
5. R. Santhanam and B. Rambabu, *Journal of Power Sources*, **195**, 5442 (2010).
6. S. Okada, M. Ueno, Y. Uebou, and J.-i. Yamaki, *Journal of Power Sources*, **146**, 565 (2005).
7. Z. Gong and Y. Yang, *Energy & Environmental Science*, **4**, 3223 (2011).
8. V. Aravindan, Y. L. Cheah, W. C. Ling, and S. Madhavi, *Journal of The Electrochemical Society*, **159**, A1435 (2012).
9. R. Sharabi, E. Markevich, V. Borgel, G. Salitra, G. Gershtinsky, D. Aurbach, G. Semrau, M. A. Schmidt, N. Schall, and C. Stinner, *Journal of Power Sources*, **203**, 109 (2012).
10. E. Markevich, R. Sharabi, H. Gottlieb, V. Borgel, K. Fridman, G. Salitra, D. Aurbach, G. Semrau, M. A. Schmidt, N. Schall, and C. Bruenig, *Electrochemistry Communications*, **15**, 22 (2012).
11. S. Amaresh, G. J. Kim, K. Karthikeyan, V. Aravindan, K. Y. Chung, B. W. Cho, and Y. S. Lee, *Physical Chemistry Chemical Physics*, **14**, 11904 (2012).
12. J. Song, D. W. Shin, Y. Lu, C. D. Amos, A. Manthiram, and J. B. Goodenough, *Chemistry of Materials*, **24**, 3101 (2012).
13. M. Jo, Y.-K. Lee, K. M. Kim, and J. Cho, *Journal of The Electrochemical Society*, **157**, A841 (2010).
14. Y.-K. Sun, Y.-S. Lee, M. Yoshio, and K. Amine, *Electrochemical and Solid-State Letters*, **5**, A99 (2002).
15. O. K. Park, Y. Cho, S. Lee, H.-C. Yoo, H.-K. Song, and J. Cho, *Energy & Environmental Science*, **4**, 1621 (2011).
16. Y. K. Sun, C. S. Yoon, and I. H. Oh, *Electrochimica Acta*, **48**, 503 (2003).
17. C. Li, H. P. Zhang, L. J. Fu, H. Liu, Y. P. Wu, E. Rahm, R. Holze, and H. Q. Wu, *Electrochimica Acta*, **51**, 3872 (2006).
18. H. M. Wu, I. Belharouak, A. Abouimrane, Y. K. Sun, and K. Amine, *Journal of Power Sources*, **195**, 2909 (2010).
19. K. S. Park, S. B. Schougaard, and J. B. Goodenough, *Advanced Materials*, **19**, 848 (2007).
20. J.-H. Park, J.-S. Kim, E.-G. Shim, K.-W. Park, Y. T. Hong, Y.-S. Lee, and S.-Y. Lee, *Electrochemistry Communications*, **12**, 1099 (2010).
21. K. Karthikeyan, S. Amaresh, V. Aravindan, H. Kim, K. S. Kang, and Y. S. Lee, *Journal of Materials Chemistry A*, **1**, 707 (2013).
22. A. Manthiram, A. Vadivel Murugan, A. Sarkar, and T. Muraliganth, *Energy and Environmental Science*, **1**, 621 (2008).
23. Y. S. Lee, Y. K. Sun, S. Ota, T. Miyashita, and M. Yoshio, *Electrochemistry Communications*, **4**, 989 (2002).
24. Y. Yang, Y. Di, X. Rui, S. Jing, T. Fuqiang, W. Xuan, and L. Qingquan, *Dielectrics and Electrical Insulation, IEEE Transactions on*, **19**, 574 (2012).
25. N. Amdouni, K. Zaghib, F. Gendron, A. Mauger, and C. M. Julien, *Ionics*, **12**, 117 (2006).
26. V. Aravindan, J. Gnanaraj, S. Madhavi, and H.-K. Liu, *Chemistry – A European Journal*, **17**, 14326 (2011).
27. A. K. Shukla and T. Prem Kumar, *Wiley Interdisciplinary Reviews: Energy and Environment*, **2**, 14 (2013).
28. V. Aravindan, K. Karthikeyan, K. S. Kang, W. S. Yoon, W. S. Kim, and Y. S. Lee, *Journal of Materials Chemistry*, **21**, 2470 (2011).